Published on 20 April 2015. Downloaded by Changchun Institute of Optics, Fine Mechanics and Physics, CAS on 29/05/2016 11:33:10.

Journal of Materials Chemistry C

ROYAL SOCIETY OF CHEMISTRY

PAPER

View Article Online
View Journal | View Issue

Cite this: J. Mater. Chem. C, 2015, 3, 5292

Received 31st January 2015, Accepted 19th April 2015

DOI: 10.1039/c5tc00317b

www.rsc.org/MaterialsC

Intense electroluminescence from ZnO nanowires

Xun Yang,[ab] Chong-Xin Shan,*[ac] Ming-Ming Jiang,[a] Jie-Ming Qin,[de] Guang-Chong Hu,[ab] Shuang-Peng Wang,[a] Hong-An Ma,[f] Xiao-Peng Jia[f] and De-Zhen Shen*[a]

Vertically aligned ZnO nanowires have been prepared, and intense electroluminescence (EL) has been observed with holes injected into the nanowires from p-type ZnO prepared *via* a high pressure high temperature route. The emission can be attributed to the radiative recombination between the electrons in the nanowires and the injected holes, and the power of the EL can reach about 10 μW when the injection current is 20 mA. The intense emission is believed to be resulted from both the relatively high quality of the nanowires and injection of the holes from the p-type ZnO.

Introduction

Zinc oxide (ZnO) has long been considered as a promising candidate for efficient ultraviolet (UV) light-emitting devices (LEDs) and low-threshold lasers due to its wide bandgap and large exciton binding energy.[1–14] However, although numerous efforts have been made, the performance of ZnO LEDs is still far below expectation. It is accepted that to realize efficient electroluminescence (EL), both a high quality active layer and efficient carrier injection are necessary. For the high quality active layer, self-assembled nanostructures usually have relatively high crystalline and optical quality. Considering that one of the most unique characteristics of ZnO lies in its rich nanostructures,[4,15–17] if the nanostructures can be employed as active layers, efficient EL from ZnO may be expected. Carrier injection is another necessity for efficient EL. It is known that ZnO is intrinsically an n-type semiconductor,[18] which means that there are many electrons, but holes are rare in this material. A natural way to achieve hole dominant conduction in ZnO is doping. However, the p-type doping of ZnO has long been a challenging issue although numerous efforts have been made.[19–23] Many methods including molecular beam epitaxy, metalorganic chemical vapor deposition, magnetron sputtering, pulsed laser deposition, *etc.* have been adopted for the p-type doping of ZnO.[24–27] However, this challenging issue has not been resolved yet, and p-type doping is still a huge barrier that hinders the realization of ZnO based LEDs. Note that the above methods employed for the p-type doping of ZnO usually run at moderate temperature and pressure. It is known that temperature and pressure are two important parameters that determine the thermal dynamics in the growth process of a material, so if high pressure high temperature can be adopted for the p-type doping of ZnO, the growth dynamics during the doping process may be altered, and surprising results may be attained. Actually, low-resistivity p-type ZnO with good stability and reproducibility has been prepared *via* a high pressure high temperature route.[28] Nevertheless, no report on LEDs using the p-type ZnO fabricated *via* such a route has been found up to now, which casts a shadow whether the p-type ZnO prepared *via* this route can be applied in optoelectronic devices.

In this paper, we show that by employing high quality ZnO nanowires as active layers of a LED, with holes injected from p-type ZnO prepared using a high pressure high temperature route, intense emission can be achieved, and the power of the emission can reach 10 μW when the injection current is 20 mA, which is amongst the best values ever reported for ZnO-based LEDs.[21] The emission is believed to be originated from the radiative recombination of the injected holes and the electrons in the ZnO nanowires.

Experimental

The ZnO nanowires were fabricated on *a*-plane sapphire using a metalorganic chemical vapor deposition technique. The precursors used for the growth of the nanowires are diethylzinc and oxygen, and high-purity (9 N) nitrogen was employed as the carrier gas to lead the precursors into the growth chamber.

[a] *State Key Laboratory of Luminescence and Applications, Changchun Institute of Optics, Fine Mechanics and Physics, Chinese Academy of Sciences, Changchun 130033, China. E-mail: shancx@ciomp.ac.cn*
[b] *University of Chinese Academy of Sciences, Beijing 100049, China*
[c] *School of Physical Engineering, Zhengzhou University, 450052, China*
[d] *School of Materials Science and Engineering, Changchun University of Science and Technology, Changchun 130022, China*
[e] *School of Physics, Inner Mongolia University for Nationalities, Tongliao 028000, China*
[f] *State Key Laboratory of Superhard Materials, Jilin University, Changchun 130012, China*

 This journal is © The Royal Society of Chemistry 2015

Published on 20 April 2015. Downloaded by Changchun Institute of Optics, Fine Mechanics and Physics, CAS on 29/05/2016 11:33:10.

Prior to the growth, the substrates were pretreated at 700 °C under 3.1×10^{-3} Pa for 30 min to remove the absorbed contaminants on the substrate surface. During the growth process, the substrate temperature was kept at 700 °C and the pressure in the chamber at 3000 Pa. The p-type ZnO employed as the hole source of the LEDs was prepared *via* a high temperature high pressure method. 99.99% ZnO powder and 99.99% Sb_2O_3 powder were mixed together uniformly, and the mole ratio of Sb_2O_3 to ZnO is 1 : 19. The mixture was pressed into a disk with a diameter of 13 mm and a height of 5 mm under 0.5 GPa, and then the disk was put into a Mo ampoule to be sintered isothermally for 15 min under 5 GPa at 1450 °C. After that, the surface layer of both sides of the disk was removed to avoid any diffusion of impurities into the sample. When the preparation of the nanowires and ZnO:Sb is finished, an indium layer was deposited onto the ZnO:Sb and the ZnO nanowires acting as electrodes in a thermal evaporation method. Then ZnO:Sb was bonded together with the nanowires by a clip to form the ZnO:Sb/n-ZnO nanowire structures.

The morphology and crystalline quality of the ZnO nanowires were characterized using a Hitachi S4800 field emission scanning electron microscope (SEM) and a FEI Tecnai F20 transmission electron microscope (TEM). The structural properties of the nanowires and ZnO:Sb were assessed using a Bruker D8 X-ray diffractometer (XRD). The photoluminescence (PL) spectra of the nanowires and ZnO:Sb were recorded using a spectrometer employing the 325 nm line of a He–Cd laser as the excitation source. The electrical properties of ZnO:Sb were measured using a Lakeshore 7707 Hall measurement system. The Sb concentration in ZnO:Sb was determined by energy-dispersive X-ray spectroscopy (EDS). Current–voltage (*I–V*) characteristics of the ZnO:Sb/n-ZnO nanowire structures were studied using an Agilent B1500A semiconductor device analyzer. Electroluminescence (EL) measurement of the structures was carried out using a Hitachi F4500 spectrometer with a continuous current power source, and the output power of the LEDs was recorded using an OPHIR Nova II power meter. The electrical potential distribution and carrier distribution in the ZnO:Sb/n-ZnO nanowire structures have been simulated using a finite difference time domain (FDTD) method.

Results and discussion

The morphology of the ZnO nanowires is shown in Fig. 1a and b. From the plan-view SEM image in Fig. 1a and the cross-sectional image in Fig. 1b, one can see that the ZnO nanowires were grown vertically on the substrate, and the nanowires are about 50 nm in diameter and 900 nm in length. Fig. 1c shows a typical TEM image of the ZnO nanowires, one can see that the nanowires have a smooth surface, symbolizing the well-crystallinity of the nanowires. A high resolution TEM image of an individual nanowire is shown in Fig. 1d. The image shows well-resolved lattice fringes, and the distance between two adjacent planes is around 0.26 nm, confirming the *c*-axis growth direction and high crystalline quality of the nanowires.

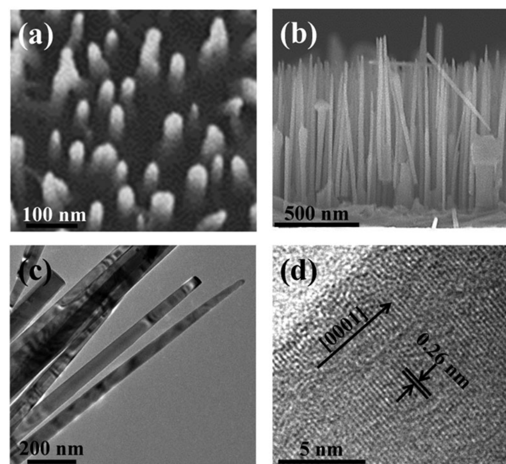

Fig. 1 Plan-view (a) and cross-sectional (b) SEM image of the ZnO nanowires; (c) TEM image of the ZnO nanowires; (d) high resolution TEM image of an individual nanowire.

Fig. 2a shows the XRD pattern of the ZnO nanowires, besides the diffraction from the sapphire substrate, only two peaks at 34.44° and 72.54° can be observed, which can be attributed to the diffraction from the (002) and (004) facets of wurtzite ZnO, respectively. The inset of Fig. 2a illustrates the X-ray rocking curve of the nanowires, and the curve shows a Gaussian shape with a full-width half-maximum (FWHM) of around 0.59°. To assess the optical

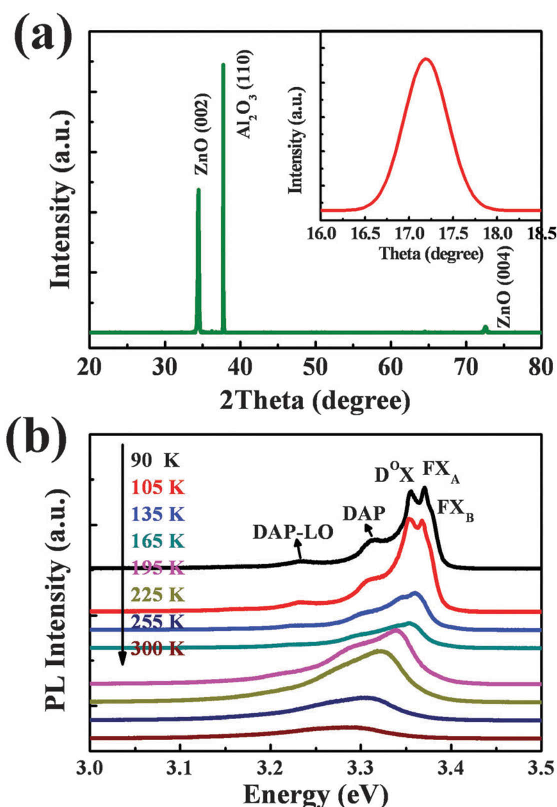

Fig. 2 (a) XRD pattern of the ZnO nanowires, and the inset shows the X-ray rocking curve of the ZnO nanowires; (b) temperature-dependent PL spectra of the ZnO nanowires.

Published on 20 April 2015. Downloaded by Changchun Institute of Optics, Fine Mechanics and Physics, CAS on 29/05/2016 11:33:10.

quality of the ZnO nanowires, temperature-dependent PL spectra from 90 K to 300 K were recorded, as shown in Fig. 2b. The 90 K PL spectrum shows four peaks at around 3.237 eV, 3.313 eV, 3.356 eV and 3.370 eV. Among these peaks, the dominant one at 3.370 eV can be attributed to the free exciton (FX_A) emission of ZnO.[29] A shoulder also appears at around 3.381 eV, which can be attributed to the emission of B-excitons in ZnO.[29] According to their positions, the peaks at 3.356 eV and 3.313 eV can be attributed to the emission from donor-bound exciton ($D^{\circ}X$) and donor–acceptor pairs (DAP).[29,30] The peak at 3.237 eV has an energy difference of 76 meV with the DAP emission, which is close to the phonon energy of ZnO (72 meV),[29] thus this peak may be the phonon replica of DAP.[30] Although free exciton emission has been frequently observed in the low-temperature PL spectra of the ZnO film and nanostructures, it is usually weak and the spectrum is usually dominated by emission from excitons localized by impurities.[29–31] The dominant free exciton emission at 90 K and the occurrence of B-exciton emission in our case reveal the high optical quality of the ZnO nanowires, which lay a solid ground for the intense emission obtained from the nanowires.

The XRD pattern of the ZnO:Sb is shown in Fig. 3a. All the prominent peaks can be attributed to the diffraction from wurtzite ZnO, while the weak peaks from antimony oxide. Note that all the peaks for ZnO:Sb shift to a smaller angle side compared with the standard peaks of ZnO, which symbolizes that Sb has been incorporated into the lattice of ZnO considering that the radius of Sb^{3+} (0.76 Å) is larger than that of Zn^{2+} (0.74 Å). Also the appearance of antimony oxide related peaks indicates that some of the Sb may precipitate out from the ZnO matrix. The morphology of ZnO:Sb is shown in Fig. 3b, and one can see that a dense layer has been formed in ZnO:Sb. Temperature-dependent PL measurements from 90 K to 300 K are also performed to investigate the optical properties of the ZnO:Sb, as shown in Fig. 3c. From the 90 K PL spectrum, three peaks can be observed at 3.361 eV, 3.316 eV, and 3.241 eV, respectively. The 3.361 eV and 3.316 eV peaks can be ascribed to the neutral acceptor bound exciton ($A^{\circ}X$) and electron transition from the conduction band to the acceptor level (FA).[28,32,33] The peak at 3.241 eV can be attributed to the DAP emission.[32,33] With the rise of temperature, the FA emission disappears gradually, while the $A^{\circ}X$ and DAP emission can still be observed from the 300 K PL spectrum at 3.288 eV (377 nm) and 3.198 eV (388 nm), respectively. The EDS spectrum of ZnO:Sb is shown in Fig. 3d, from which only the signals for Zn, O and Sb can be observed, and the Sb content in ZnO:Sb is about 4.38 atom%, in a rough agreement with the mole ratio of Sb_2O_3 to ZnO in the precursors (1 : 19).

To act as the hole source for the ZnO nanowires, ZnO:Sb should have relatively high hole concentration. To assess the hole concentration of the ZnO:Sb, Hall measurement has been carried out. It is revealed that ZnO:Sb exhibits p-type conduction, with the room temperature hole concentration and Hall mobility of 3.8×10^{19} cm^{-3} and 1.9 cm^2 V^{-1} s^{-1}, respectively. Similar results have been reported previously,[28] and the origin of the p-type conductivity in ZnO:Sb is usually attributed to the formation of Sb_{Zn}–$2V_{Zn}$ complexes.[34] Such a high hole concentration is favorable for acting as a hole source.

To inject holes into the ZnO nanowires, p-ZnO:Sb has been bonded together with the ZnO nanowires by a clip to form the p-ZnO:Sb/n-ZnO nanowire structures. Fig. 4a shows the schematic illustration of the structure. The structure exhibits an obvious rectifying characteristic with a turn-on voltage of about 4.6 V, as shown in Fig. 4b. The inset of Fig. 4b shows the *I–V* curves for In contact on the p-ZnO:Sb and n-ZnO nanowires. The linear curves reveal that ohmic contacts have been obtained in both cases, indicating that the rectifying effect comes from

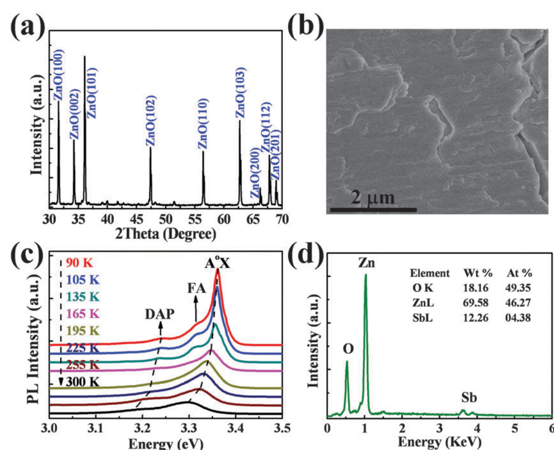

Fig. 3 XRD pattern (a); SEM image (b); temperature-dependent PL spectra (c), and EDS spectrum (d) of the ZnO:Sb sample.

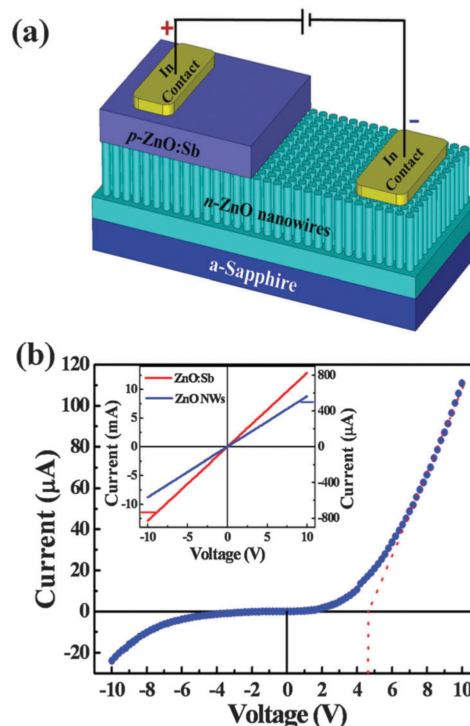

Fig. 4 (a) Schematic illustration of the p-ZnO:Sb/n-ZnO nanowire structure; (b) *I–V* curve of the p-ZnO:Sb/n-ZnO nanowire structure, the inset shows the *I–V* curves of the In contact on the n-ZnO nanowires and the p-ZnO:Sb.

This journal is © The Royal Society of Chemistry 2015

Published on 20 April 2015. Downloaded by Changchun Institute of Optics, Fine Mechanics and Physics, CAS on 29/05/2016 11:33:10.

p–n junctions formed between the p-ZnO:Sb and the n-ZnO nanowires.

To test the application of the structure in LEDs, a forward bias has been applied onto the structure, and purple emission can be observed clearly, as indicated in Fig. 5. Fig. 5a shows the typical optical image of the device, and the output power can reach 10 μW when the injection current is 20 mA (with a bias voltage of around 85 V), which is amongst the highest values ever reported for ZnO-based LEDs.[21,35] The EL spectra of the device are shown in Fig. 5b. There is a dominant emission band at around 396 nm, and another weak emission at around 500 nm is also visible. The dominant emission can be attributed to the NBE emission, while the weak one to the deep-level related emission of ZnO.

To explore the origin of the EL emission, the room temperature PL spectra of the ZnO nanowires and ZnO:Sb have been recorded, as shown in Fig. 5c. It can be found that the PL spectrum of the ZnO nanowires shows a strong peak at around 377 nm, while the deep-level emission is almost undetectable. Nevertheless, the spectrum of the p-ZnO:Sb sample is dominated by the deep-level related emission of ZnO, while the NBE emission of ZnO is weak. Note that there appear two peaks for the NBE emission of ZnO:Sb, and the peak at 377 nm can be attributed to the acceptor bound excitonic emission of ZnO, and the shoulder at 388 nm is from the DAP emission based on the temperature dependent PL spectra shown in Fig. 3c. One can see from Fig. 5 that the EL spectra of the p-ZnO:Sb/n-ZnO nanowire structure are similar in shape to the PL spectrum of the ZnO nanowires although the peak position is slightly different, thus the EL emission in the structure may come from the radiative recombination of electrons and holes in the ZnO nanowires.

In order to understand the emission mechanism of the p-ZnO:Sb/n-ZnO nanowire structures better, the distribution of charge carriers and electric potential in the p-ZnO:Sb/n-ZnO structure under forward bias has been simulated using the FDTD method, as illustrated in Fig. 6. In the p-ZnO:Sb/n-ZnO nanowire structures, since the hole concentration of ZnO:Sb (3.8×10^{19} cm^{-3}) is much higher than the electron concentration in the nanowires (usually in the order of 10^{16} cm^{-3}), the depletion area of the p–n junction will be distributed mainly in the nanowires, as indicated in Fig. 6a. The carrier distribution in the p-ZnO:Sb/n-ZnO nanowire structure is shown in Fig. 6b, one can see that the holes in the p-ZnO:Sb can be injected into the ZnO nanowires. Therefore, the injected holes will recombine with the electrons in the ZnO nanowires, and electroluminescence from the ZnO nanowires will be detected. The relatively high structural and optical quality of the nanowires may facilitate the occurrence of near ultraviolet emission. As for the slight redshift of the EL position compared with the NBE emission of ZnO, it may come from the heating effect caused by the injection of continuous current. Note that no report on ZnO LEDs using p-type ZnO prepared *via* a high pressure high temperature method has been demonstrated before.

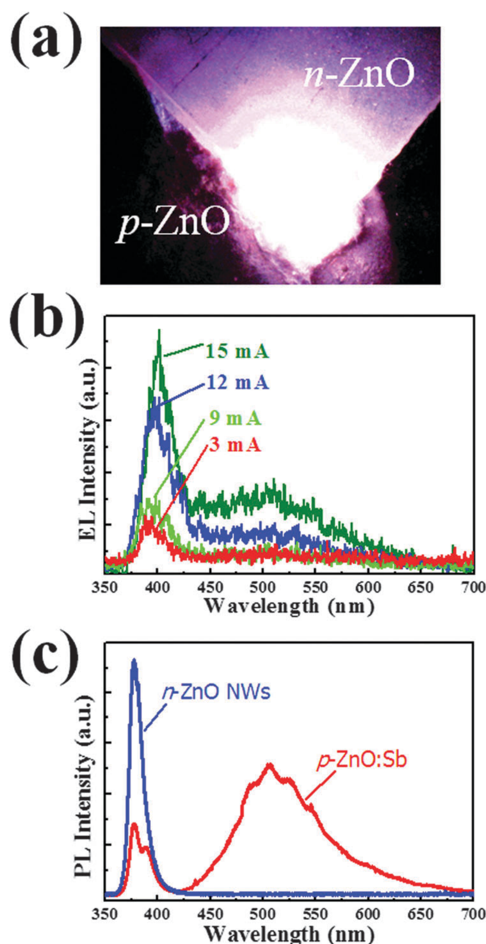

Fig. 5 Optical image (a) and EL spectra (b) of the p-ZnO:Sb/n-ZnO nanowire structure; (c) room temperature PL spectra of the n-ZnO nanowires and p-ZnO:Sb.

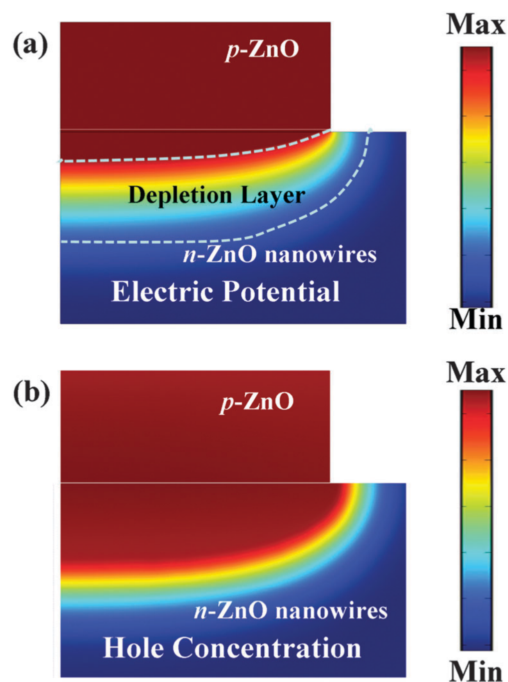

Fig. 6 Spatial distribution of the electric potential (a) and hole concentration (b) in the p-ZnO:Sb/n-ZnO nanowire structure.

View Article Online

Published on 20 April 2015. Downloaded by Changchun Institute of Optics, Fine Mechanics and Physics, CAS on 29/05/2016 11:33:10.

Conclusions

In summary, ZnO nanowires have been prepared, and with holes injected from p-ZnO:Sb fabricated *via* a high pressure and high temperature route, bright emission has been observed. The output power can reach around 10 μW when the injection current is 20 mA, which is amongst the best values ever reported for ZnO LEDs. The intense emission can be attributed to the relative high structural and optical quality of the nanowires and the relatively high hole concentration of the ZnO:Sb layer. The results reported here may provide a facile route to high performance ZnO electroluminescence.

Acknowledgements

This work was financially supported by the National Basic Research Program of China (2011CB302005), the National Science Foundation for Distinguished Young Scholars of China (61425021), the Natural Science Foundation of China (11134009, 11404328, 11374296, 11464035 and 61177040), and the Science and Technology Developing Project of Jilin Province (20111801 and 20140101052JC).

Notes and references

1 H. Zhu, C. X. Shan, B. Yao, B. H. Li, J. Y. Zhang, Z. Z. Zhang, D. X. Zhao, D. Z. Shen, X. W. Fan, Y. M. Lu and Z. K. Tang, *Adv. Mater.*, 2009, **21**, 1613.
2 G. Y. Zhu, C. X. Xu, L. S. Cai, J. T. Li, Z. L. Shi, Y. Lin, G. F. Chen, T. Ding, Z. S. Tian and J. Dai, *ACS Appl. Mater. Interfaces*, 2012, **4**, 6195–6201.
3 P. N. Ni, C. X. Shan, S. P. Wang, X. Y. Liu and D. Z. Shen, *J. Mater. Chem. C*, 2013, **1**, 4445–4449.
4 H. X. Dong, Y. Liu, J. Lu, Z. H. Chen, J. Wang and L. Zhang, *J. Mater. Chem. C*, 2013, **1**, 202–206.
5 J. Huang, S. Chu, J. Y. Kong, L. Zhang, C. M. Schwarz, G. P. Wang, L. Chernyak, Z. H. Chen and J. L. Liu, *Adv. Opt. Mater.*, 2013, **1**, 179–185.
6 G. Lozano, D. J. Louwers, S. R. K. Rodrıguez, S. Murai, O. T. Jansen, M. A. Verschuuren and J. G. Rivas, *Light: Sci. Appl.*, 2013, **2**, e66.
7 Q. Qiao, C. X. Shan, J. Zheng, H. Zhu, S. F. Yu, B. H. Li, Y. Jia and D. Z. Shen, *Nanoscale*, 2013, **5**, 513–517.
8 X. Y. Liu, C. X. Shan, S. P. Wang, H. F. Zhao and D. Z. Shen, *Nanoscale*, 2013, **5**, 7746–7749.
9 S. L. Li and L. C. Zhang, *J. Semicond.*, 2013, **34**, 114010.
10 X. Z. Zhang, X. J. Zhang, J. B. Xu, X. D. Shan, J. Xu and D. P. Yu, *Opt. Lett.*, 2009, **34**, 2533–2535.
11 X. M. Mo, G. J. Fang, H. Long, S. Z. Li, H. H. Huang, H. N. Wang, Y. H. Liu, X. Q. Meng, Y. P. Zhang and C. X. Pan, *J. Lumin.*, 2013, **137**, 116–120.
12 S. Z. Li, W. W. Lin, G. J. Fang, F. Huang, H. H. Huang, H. Long, X. M. Mo, H. N. Wang, W. J. Guan and X. Z. Zhao, *J. Lumin.*, 2013, **140**, 110–113.
13 X. M. Mo, G. J. Fang, H. Long, S. Z. Li, H. N. Wang, Z. Chen, H. H. Huang, W. Zeng, Y. P. Zhang and C. X. Pan, *Phys. Chem. Chem. Phys.*, 2014, **16**, 9302–9308.
14 Y. Yang, X. W. Sun, B. K. Tay, G. F. You, S. T. Tan and K. L. Teo, *Appl. Phys. Lett.*, 2008, **93**, 253107.
15 K. Mahmood, S. B. Park and H. J. Sung, *J. Mater. Chem. C*, 2013, **1**, 3138–3149.
16 C. K. Xu, P. Shin, L. L. Cao and D. Gao, *J. Phys. Chem. C*, 2010, **114**, 125–129.
17 H. M. Cheng, W. H. Chiu, C. H. Lee, S. Y. Tsai and W. F. Hsieh, *J. Phys. Chem. C*, 2008, **112**, 16359–16364.
18 S. B. Zhang, S. H. Wei and A. Zunger, *Phys. Rev. B*, 2001, **63**, 075205.
19 S. J. Jiao, Z. Z. Zhang, Y. M. Lu, D. Z. Shen, Y. Yao, J. Y. Zhang, B. H. Li, D. X. Zhao, X. W. Fan and Z. K. Tang, *Appl. Phys. Lett.*, 2006, **88**, 031911.
20 A. Tsukazaki, A. Ohtomo, T. Onuma, M. Ohtani, T. Makino, M. Sumiya, K. Ohtani, S. F. Chichibu, S. Fuke, Y. Segawa, H. Ohno, H. Koinuma and M. Kawasaki, *Nat. Mater.*, 2005, **4**, 42–46.
21 K. Nakahara, S. Akasaka, H. Yuji, K. Tamura, T. Fujii, Y. Nishimoto, D. Takamizu, A. Sasaki, T. Tanabe, H. Takasu, H. Amaike, T. Onuma, S. F. Chichibu, A. Tsukazaki, A. Ohtomo and M. Kawasaki, *Appl. Phys. Lett.*, 2010, **97**, 013501.
22 J. C. Fan, C. Y. Zhu, S. Fung, Y. C. Zhong, K. S. Wong, Z. Xie, G. Brauer, W. Anwand, W. Skorupa, C. K. To, B. Yang, C. D. Beling and C. C. Ling, *J. Appl. Phys.*, 2009, **106**, 073709.
23 H. Shen, C. X. Shan, J. S. Liu, B. H. Li, Z. Z. Zhang and D. Z. Shen, *Phys. Status Solidi B*, 2013, **250**, 2102–2105.
24 D. C. Look, D. C Reynolds, C. W. Litton, R. L. Jones, D. B. Eason and G. Cantwell, *Appl. Phys. Lett.*, 2002, **81**, 1830–1832.
25 Y. Ma, G. T. Du, S. R. Yang, Z. T. Li, B. J. Zhao, X. T. Yang, T. P. Yang, Y. T. Zhang and D. L. Liu, *J. Appl. Phys.*, 2004, **95**, 6268–6272.
26 Y. J. Zeng, Z. Z. Ye, W. Z. Xu, D. Y. Li, J. G. Lu, L. P. Zhu and B. H. Zhao, *Appl. Phys. Lett.*, 2006, **88**, 062107.
27 M. S. Oh, S. H. Kim and T. Y. Seong, *Appl. Phys. Lett.*, 2005, **87**, 122103.
28 J. M. Qin, B. Yao, Y. Yan, J. Y. Zhang, X. P. Jia, Z. Z. Zhang, B. H. Li, C. X. Shan and D. Z. Shen, *Appl. Phys. Lett.*, 2009, **95**, 022101.
29 J. N. Dai, H. C. Liu, W. Q. Fang, L. Wang, Y. Pu, Y. F. Chen and F. Y. Jiang, *J. Cryst. Growth*, 2005, **283**, 93–99.
30 C. X. Shan, Z. Liu and S. K. Hark, *Appl. Phys. Lett.*, 2008, **92**, 073103.
31 S. S. Kurbanov, H. D. Cho and T. W. Kang, *Opt. Commun.*, 2011, **284**, 240–244.
32 F. X. Xiu, Z. Yang, L. J. Mandalapu, D. T. Zhao and J. L. Liu, *Appl. Phys. Lett.*, 2005, **87**, 252102.
33 X. Fang, J. H. Li, D. X. Zhao, B. H. Li, Z. Z. Zhang, D. Z. Shen, X. H. Wang and Z. P. Wei, *Thin Solid Films*, 2010, **518**, 5687–5689.
34 S. Limpijumnong, S. B. Zhang, S. H. Wei and C. H. Park, *Phys. Rev. Lett.*, 2004, **92**, 155504.
35 H. Kato, T. Yamamuro, A. Ogawa, C. Kyotani and M. Sano, *Appl. Phys. Express*, 2011, **4**, 091105.

 This journal is © The Royal Society of Chemistry 2015